European Journal of Medicinal Chemistry 184 (2019) 111745

Contents lists available at ScienceDirect

European Journal of Medicinal Chemistry

journal homepage: http://www.elsevier.com/locate/ejmech

Research paper

Design and synthesis of H_2S-donor hybrids: A new treatment for Alzheimer's disease?

Simona Sestito [a], Letizia Pruccoli [b], Massimiliano Runfola [a], Valentina Citi [a], Alma Martelli [a, c, d], Giuseppe Saccomanni [a], Vincenzo Calderone [a, c, d], Andrea Tarozzi [b, **], Simona Rapposelli [a, d, *]

[a] Department of Pharmacy, University of Pisa, Italy
[b] Department for Life Quality Studies, University of Bologna, Italy
[c] Interdepartmental Research Centre "Nutraceuticals and Food for Health (NUTRAFOOD)", University of Pisa, Italy
[d] Interdepartmental Research Centre of Ageing Biology and Pathology, University of Pisa, Italy

ARTICLE INFO

Article history:
Received 23 July 2019
Received in revised form
12 September 2019
Accepted 26 September 2019
Available online 27 September 2019

Keywords:
Hydrogen sulphide
Multitarget approach
Alzheimer's disease
Sulforaphane
Erucin

ABSTRACT

Hydrogen sulphide (H_2S) is an endogenous gasotransmitter, largely known as a pleiotropic mediator endowed with antioxidant, anti-inflammatory, pro-autophagic, and neuroprotective properties. Moreover, a strong relationship between H_2S and aging has been recently identified and consistently, a significant decline of H_2S levels has been observed in patients affected by Alzheimer's disease (AD). On this basis, the use of H_2S-donors could represent an exciting and intriguing strategy to be pursued for the treatment of neurodegenerative diseases (NDDs).

In this work, we designed a small series of multitarget molecules combining the rivastigmine-scaffold, a well-established drug already approved for AD, with sulforaphane (SFN) and erucin (ERN), two natural products deriving from the enzymatic hydrolysis of glucosinolates contained in broccoli and rocket, respectively, endowed both with antioxidant and neuroprotective effects.

Notably, all new synthetized hybrids exhibit a H_2S-donor profile *in vitro* and elicit protective effects in a model of LPS-induced microglia inflammation. Moreover, a decrease in NO production has been observed in LPS-stimulated cells pre-treated with the compounds. Finally, the compounds showed neuroprotective and antioxidant activities in human neuronal cells. The most interesting compounds have been further investigated to elucidate the possible mechanism of action.

1. Introduction

Hydrogen sulphide (H_2S) is an endogenous gasotransmitter, which acts as a signaling molecule in the central nervous system (CNS) as well as in many other districts. In the CNS it is mainly produced by cystathionine β-synthase (CBS) by the use of the amino acids L-cysteine and homocysteine as substrates. Altered levels of CBS have been found in subjects affected by neurodegenerative diseases. For instance, in patients affected by Alzheimer's disease (AD) the expression of CBS is drastically decreased, resulting in a significant decline of H_2S levels [1]. Basically, H_2S has emerged as a pleiotropic mediator endowed with antioxidant [2], anti-inflammatory [3], pro-autophagic [4] and neuroprotective properties [5]. The existence of a strong relationship between H_2S and aging [6] has been proved for the first time in *C. elegans* in which the exposure to low concentrations of exogenous H_2S induced beneficial effects on lifespan [7]. Up to date, the design of new H_2S-donors as novel pharmacological agents for the treatment of neurodegenerative diseases (NDDs) represents an exciting and intriguing task to be pursued.

As for many others NDDs characterized by a complex etiology, the treatment of AD still represents one of the major therapeutic areas where the discovery of new effective drugs remains a major challenge. To date, scientists are currently taking advantage of the 'multi-target approach' as a promising option to develop new drugs for the treatment of AD [8–10]. Consistently, in the last decade our group made big efforts in the development of therapeutically useful

* Corresponding author. Department of Pharmacy, University of Pisa, Italy.
** Corresponding author.
E-mail addresses: andrea.tarozzi@unibo.it (A. Tarozzi), simona.rapposelli@unipi.it (S. Rapposelli).

https://doi.org/10.1016/j.ejmech.2019.111745
0223-5234/

molecules for NDD following this approach [11–13]. In particular, we have recently synthetized the first neuroprotective H_2S-hybrid agent by combining the molecular scaffold of memantine (NMDA antagonist) with an isothiocyanate group able to release H_2S through a cysteine-mediated mechanism, thus generating memantine [14]. To further expand the class of new H_2S-releasing agents we developed new chemical entities based on the combination of rivastigmine an acetylcholinesterase (AChE) inhibitor with brain-region selectivity [15] and FDA approved for AD, with antioxidant natural products. In particular, we identified sulforaphane (SFN) and erucin (ERN), mainly deriving from broccoli and rocket glucosinolates, as two interesting compounds to be included in the design of new H_2S-hybrids [16] (Fig. 1). Several studies revealed the therapeutic and prophylactic properties of both SFN and ERN [17,18], including strong antioxidant [19,20], anti-inflammatory activity and neuroprotective effects [21]. The pleiotropic role of both isothiocyanates has been linked to their ability to address several targets (i.e. NO, GSH, Nrf2/ARE pathway) and to modulate different pathways in neuronal and glial cells [22].

Within the complexity and multifactorial etiology of AD, hyperactivation of microglia has emerged as a pivotal player in the pathogenesis of late AD. The significant reduction of cholinergic neurotransmission promotes microglial activation and subsequently, the release of pro-inflammatory factors [23]. Moreover, the close correlation between the inflammatory state of microglia and the severity of neurodegeneration [24–26] suggests microglia's inflammation as a consistent biological target.

With the aim to design new protective agents against neuronal inflammation and able to induce a substantial drop in ROS production, we synthesized original H_2S-releasing hybrids combining the rivastigmine-scaffold with SFN/ERN pharmacophores through a multitarget approach. The present work deals with the design and synthesis of new multitarget chemical entities, and with the evaluation of their biological profile. In particular, we evaluated their capability to release H_2S and to elicit protective effects in a model of LPS-induced inflammation of microglia. We also assessed the effects induced on NO-production. In addition, the neuroprotective and antioxidant activities in human neuronal cells have been determined. The most interesting compounds have been further investigated to elucidate the potential mechanism of action.

2. Materials and Methods

2.1. Chemistry

The synthesis of the final products 1–6 was carried out following the synthetic procedure showed in Scheme 1. The reaction between phthalimide potassium 7 and 1,4-dibromobutane in acetone gave the bromo-derivative 8, which was then reacted with potassium thioacetate in THF to give the thioester 9. The following hydrolysis furnished the thiol 10 which was alkylated with the appropriate chloroacetamide 11a-c [27] in the presence of KOH to afford the corresponding thioethers 12–14. The subsequent hydrazinolysis provided respectively the intermediates 15–17, which were treated with thiophosgene and NaOH to give the isothiocyanates 1–3. Finally, oxidation of compounds 1–3 by Oxone® led to sulphoxides 4–6.

3. Results and discussion

3.1. H_2S-release and anti-inflammatory effects in microglia BV-2 cells

Intracellular H_2S-release of compounds 1–6 was tested in a murine microglia cell line (BV-2) using WSP-1, a fluorescent dye indicating the generation of intracellular H_2S [28]. Administration of 100 μM of the tested compounds to BV-2 caused a significant increase in WSP-1 fluorescence levels reaching the plateau in about 45 min. Concentration of 100 μM was selected according to dye manufacturer, due to its relatively short time of recording. The area under the curve (AUC) of the H_2S-release (expressed as fluorescence index, FI) was calculated for each compound, and the amount

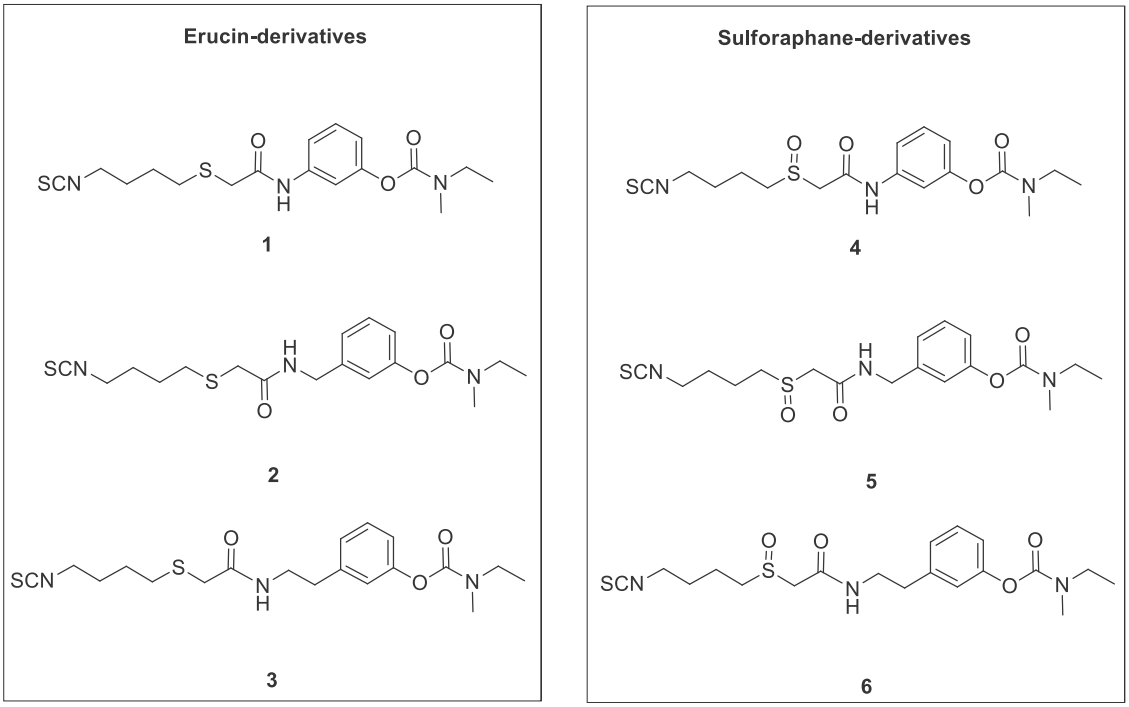

Fig. 1. Structures of ERN and SFN-rivastigmine hybrids.

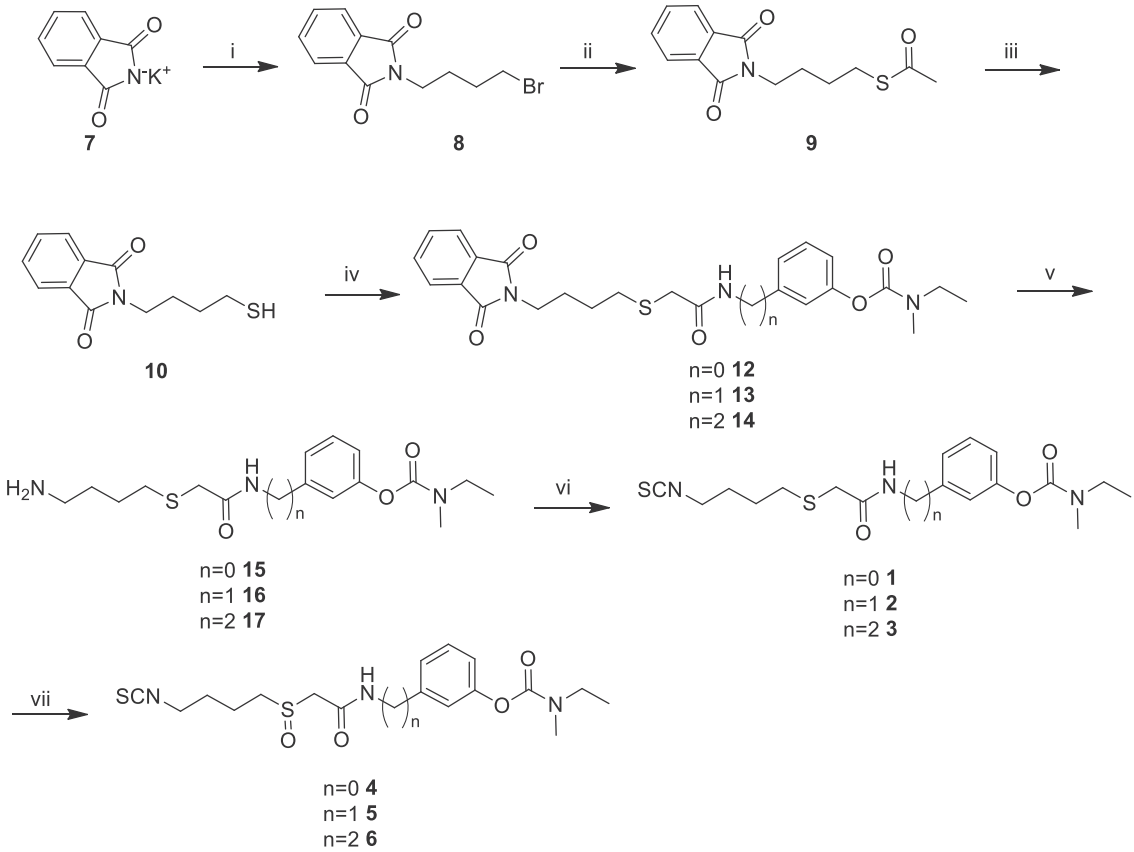

Scheme 1. Reagents and conditions: i) 1,4-dibromobutane, acetone, reflux, 12 h; ii) MeCOS−K^+, THF, reflux, 12 h; iii) HCl 37%, MeOH, reflux, 12 h; iv) 11a-c, KOH, acetone, reflux, 12 h; v) $NH_2NH_2 \times H_2O$, EtOH, reflux, 1 h; vi) thiophosgene, NaOH, DCM, r.t., vii) Oxone/H_2O, MeOH/THF (1:1), r.t., 1 h.

of H_2S released from the hybrid compounds and native molecule rivastigmine, as negative control, were compared with H_2S levels produced by 100 μM of diallyl disulfide (DADS), a well-known slow H_2S-donor. All tested compounds exhibited a slow H_2S-donor profile. Moreover, the amount of H_2S generated by almost all the hybrid compounds, was comparable to diallyl disulfide (DADS), except for compound 2 which exhibited the highest levels of intracellular H_2S-release (Fig. 2).

Isothiocyanates like ERN and SFN were described as H_2S-donors in several previous works [29–32]. Remarkably, H_2S exhibits two opposite concentration-dependent behaviors. This feature, named "*hormesis*", consists in a protective and pro-proliferative effect at low concentrations that switch to anti-proliferative and anti-cancer ones at high concentrations [33]. Hence, the new hybrids and rivastigmine were tested at the concentration of 1 μM to evaluate their cytoprotective effect on microglial cells against LPS- induced

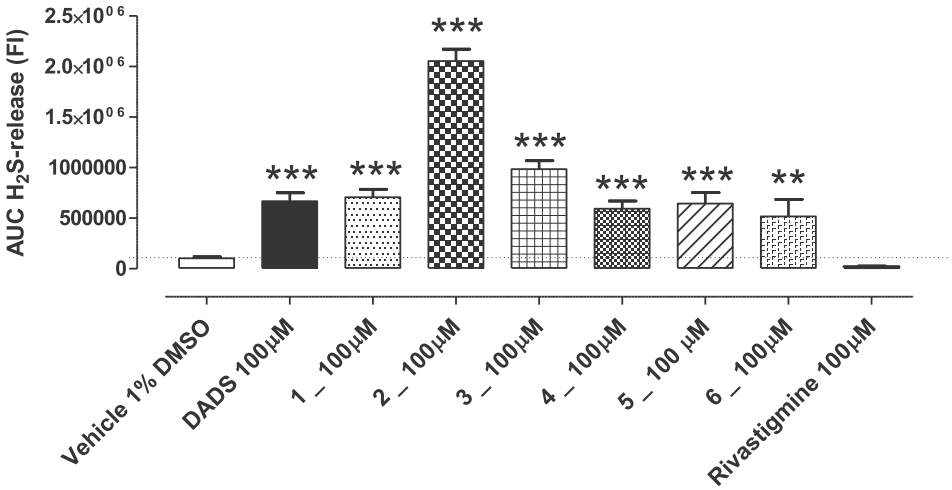

Fig. 2. Intracellular H_2S-release in BV-2 cells. The histograms show the total amount of H_2S released by vehicle, DADS and the tested compounds (1–6) 100 μM during 45 min, expressed as AUC. The vertical bars represent the standard error (n = 9). The asterisks indicate a statistically significant difference from vehicle (**$p < 0.01$ and ***$p < 0.001$ vs vehicle). Cell viability in microglia BV-2 cells.

neuroinflammatory stimuli. The administration of LPS (5 μg/ml for 24 h) to BV2 cells, led to approximately a 20% decrease in cell viability (80.6 ± 1.2%). The pre-incubation of almost all the tested compounds, except compound 6, induced a significant reduction of LPS-induced damage preserving cell viability. In particular, the native compound rivastigmine induced a slight although significant increase in cell viability (84.0 ± 1.0%) but, notably, the 1 h pre-incubation with all hybrid compounds led to a further increase in BV-2 viability, compared both to LPS treated cells and rivastigmine pre-incubation. In particular, this increase reached a statistical significance for compound 1 (93.0 ± 3.2%) (Fig. 3).

A typical effect of a sub-clinic inflammation is represented by the increase in ROS production in cells subjected to pro-inflammatory stimuli [34]. Accordingly, a 24 h LPS administration elicited a significant increase of ROS vs vehicle (154 ± 3.8%) in BV-2 cell lines. All the tested compounds, except rivastigmine, exhibited a clear antioxidant effect with a significant reduction of ROS of about 30–35% after 1 h of pre-incubation and 24 h of co-incubation with LPS. Rivastigmine did not show any significant effect on LPS-induced ROS increase (Fig. 4).

The LPS-induced neuroinflammation or other pro-inflammatory stimuli leads to an increase in nitric oxide levels inside cells as marker of inflammation. In particular, the incubation of BV-2 with LPS for 24 h in our experimental protocol induced a significant increase of NO levels of about 46% (145.7 ± 4.4%) compared to vehicle. This increase was counteracted by all the tested compounds even if only hybrid compounds 1 (117.4 ± 11.9%), 2 (125.9 ± 6.9%), and 3 (98.8 ± 26.5%) led to a significant decrease of NO levels (Fig. 5). Although further investigations are required, we can speculate that the different decrease in NO levels observed for ERN- and SFN-derivatives could be affected by the H_2S-releasing properties.

The neurotoxicity of compounds 1, 2 and 4–6 was evaluated in SH-SY5Y cells using the MTT assay. The 24 h incubation with different concentrations of the tested compounds (1.25–40 μM) recorded that concentrations up to 5 μM did not affect the neuronal viability (data not shown). Therefore, all the hybrids were used at the maximum concentration of 5 μM in the following experiments.

To investigate the antioxidant activity in terms of inhibition of intracellular ROS, SH-SY5Y cells were incubated with the tested compounds for 24 h and then with hydrogen peroxide (H_2O_2) or *tert*-butyl hydroperoxide (*t*-BuOOH) for 30 min. The ROS formation in SH-SY5Y cells was evaluated using the fluorescent probe 2′–7′ dichlorodihydrofluorescein diacetate (DCFH-DA). Compounds 1 and 2 showed the highest antioxidant activity against the ROS formation elicited by both H_2O_2 and *t*-BuOOH (Fig. 6). To understand the molecular mechanisms involved in the antioxidant activity, we evaluated the ability of hybrid compounds to induce the formation of the antioxidant mediator glutathione (GSH).

The GSH levels in SH-SY5Y cells were evaluated after 24 h of incubation with the hybrid compounds 1, 2 and 4–6 (5 μM) using the fluorescent probe monochlorobimane (MCB). As depicted in Fig. 7, compounds 1 and 2 recorded the best capacity to increase the basic levels of GSH with an increase percentage of 35.60% and 25.73%, respectively. We speculated that this effect could be related to activation of Nrf2 pathway, as previously reported for SFN and ERN [35]. Thus, we decided to assess the capacity of the hybrid compounds 1 and 2 to activate the Nrf2 pathway which is a transcription factor that once activated binds to the antioxidant response element (ARE), thus initiating the transcription of cytoprotective genes.

In particular, the Nrf2 activation at nuclear level in SH-SY5Y cells, was evaluated using the TransAM Nrf2 kit after different times of incubation with compounds 1 and 2. Only compound 1 was able to activate Nrf2 suggesting that its antioxidant activity is due to an increase of genetic transcription of GSH (Fig. 8).

The neuroprotective activity against the neurotoxicity induced by $A\beta_{1-42}$ oligomers ($OA\beta_{1-42}$) in SH-SY5Y cells was also evaluated after 24 h of incubation with the hybrid compounds 1, 2 and 4–6 (5 μM) and 4 h of incubation with $OA\beta_{1-42}$ using the MTT formazan exocytosis assay. All the tested compounds did not exert neuroprotective effects against the neurotoxicity induced by $OA\beta_{1-42}$ (see SI).

This result confirms that the neuroprotective effects observed for the new hybrid compounds are finely due to the H_2S-releasing properties and not to a direct inhibition of the Aβ-aggregation.

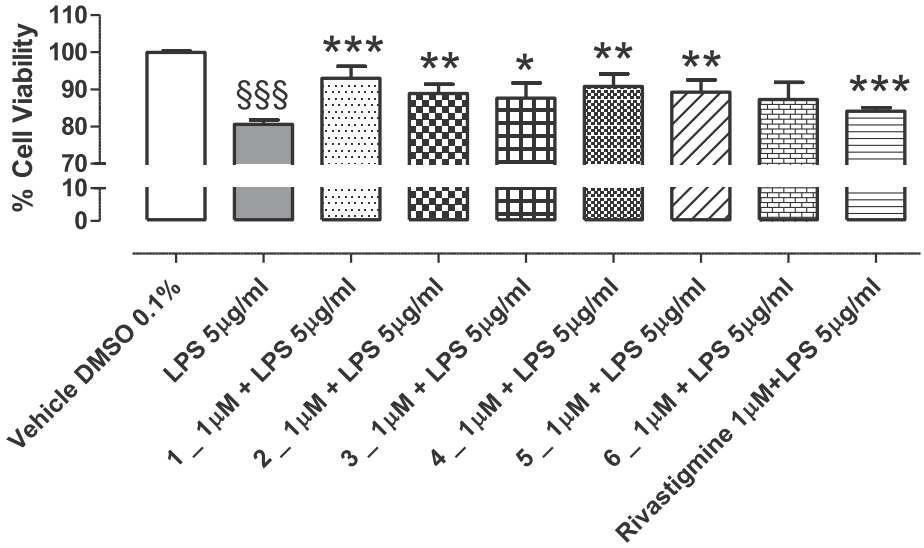

Fig. 3. The histograms show the viability of BV-2 cells treated with vehicle, LPS 5 μg/ml, tested compounds + LPS 5 μg/ml (1–6) or rivastigmine 1 μM. Data are expressed as a percentage of viability recorded for BV-2 cells treated with vehicle. The vertical bars represent the standard error (n = 9). The § indicate a statistically significant difference from vehicle (§§§$p < 0.001$) The asterisks indicate a statistically significant difference from LPS 5 μg/ml (*$p < 0.05$, **$p < 0.01$, ***$p < 0.001$). ROS production in microglia BV-2 cells.

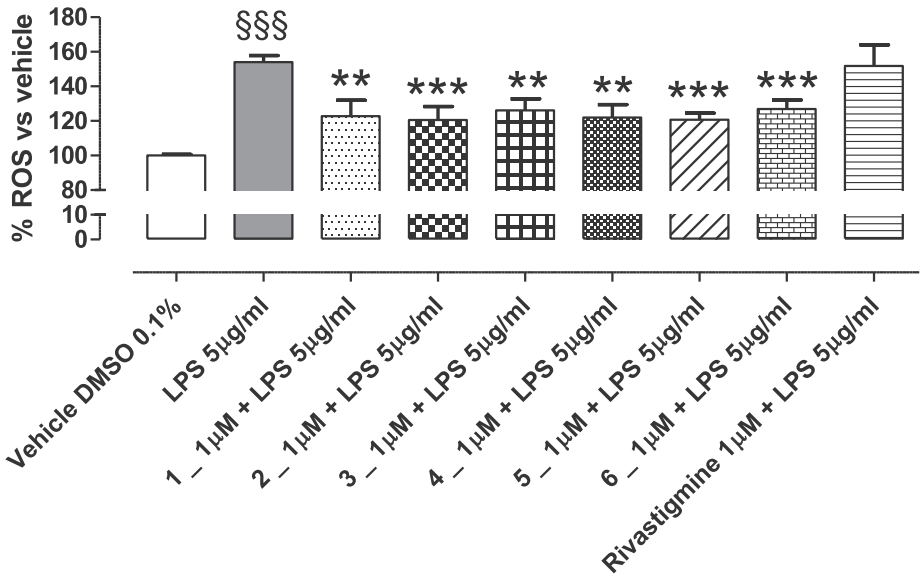

Fig. 4. The histograms show the ROS amount of BV-2 cells treated with vehicle, LPS 5 μg/ml, tested compounds + LPS 5 μg/ml (1–6) or rivastigmine 1 μM. Data are expressed as a percentage of ROS production recorded for BV-2 cells treated with vehicle. The vertical bars represent the standard error (n = 9). The § indicate a statistically significant difference from vehicle (§§§$p < 0.001$). The asterisks indicate a statistically significant difference from LPS 5 μg/ml (**$p < 0.01$ and ***$p < 0.001$). NO formation in microglia BV-2 cells.

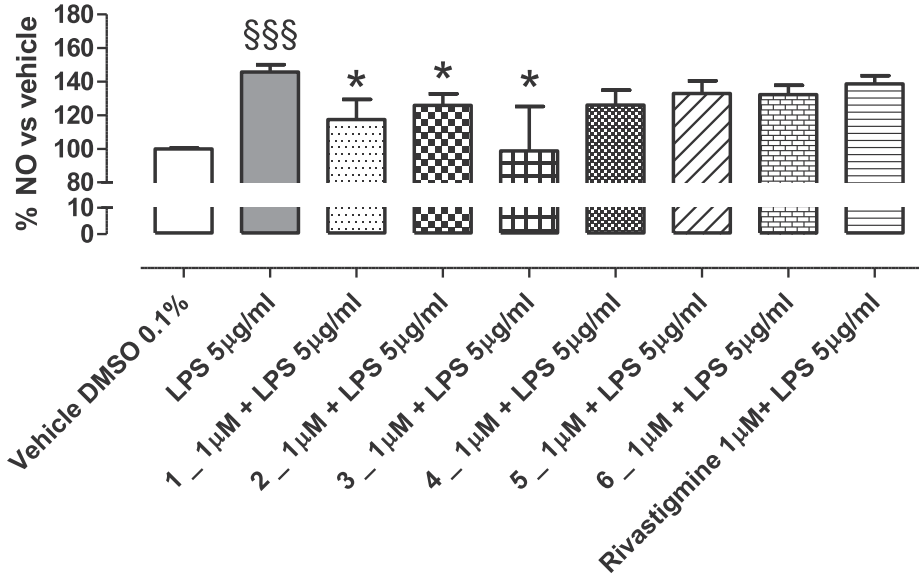

Fig. 5. The histograms show the NO amount of BV-2 cells treated with vehicle, LPS 5 μg/ml, tested compounds + LPS 5 μg/ml (1–6) or rivastigmine 1 μM. Data are expressed as a percentage of NO production recorded for BV-2 cells treated with vehicle. The vertical bars represent the standard error (n = 9). The § indicate a statistically significant difference from vehicle (§§§$p < 0.001$) The asterisks indicate a statistically significant difference from LPS 5 μg/ml (*$p < 0.05$). Antioxidant and neuroprotective effects in neuronal SH-SY5Y cells.

3.2. Determination of lipophilicity

Brain selectivity is strongly related to the specific capability of a drug to cross BBB. Therefore, since lipophilicity represents one of the main requirements requested to address this issue, especially in AD, we predicted the theoretical logP of compounds 1–6 (Table 1) compared with their native drug. Calculations revealed that compounds 1–3 possess a logP higher than rivastigmine (logP = 2,41), already described as drug with brain oriented selectivity [15]. Even if these theoretical data are only preliminary, we hypothesise that the new compounds could be able to cross the BBB and exert a neuroprotective and H_2S-mediated effect on both neuronal and microglia cells.

4. Conclusions

The goal of our study was to develop and preliminarily evaluate a new class of multitarget H_2S-donor hybrids. These new chemical

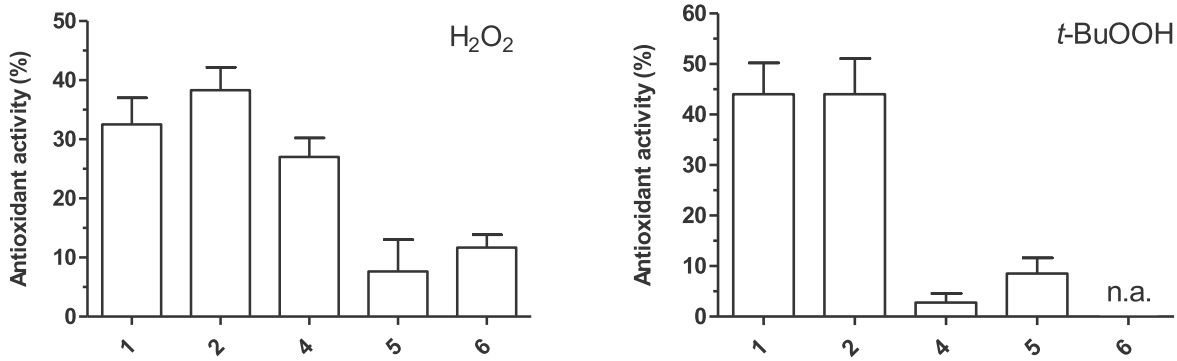

Fig. 6. Antioxidant activity of compounds 1, 2 and 4–6 against the ROS formation induced by H_2O_2 or *t*-BuOOH in SH-SY5Y cells. Cells were incubated with the tested compounds (5 μM) for 24 h and then with H_2O_2 or *t*-BuOOH (50 μM) for 30 min. At the end of incubation, intracellular ROS formation was detected using the fluorescent probe DCFH-DA, as described in the Materials and Methods section. Data are expressed as antioxidant activity in terms of inhibition percentage of ROS formation induced by H_2O_2 or *t*-BuOOH and reported as mean ± SEM of three independent experiments; n.a. = not active. Effects induced on GSH levels in neuronal SH-SY5Y cells.

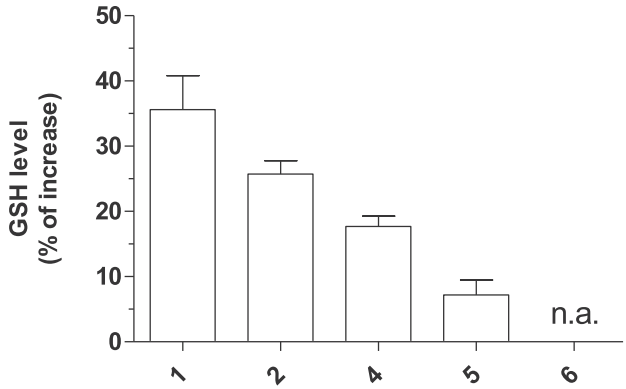

Fig. 7. Effects of compounds 1, 2 and 4–6 on GSH levels in SH-SY5Y cells. Cells were incubated with the tested compounds (5 μM) for 24 h. At the end of incubation, GSH levels were detected using the fluorescent probe MCB, as described in the Materials and Methods section. Data are expressed as increase percentage of GSH level and reported as mean ± SEM of three independent experiments; n.a. = not active.

entities were obtained combining natural occurring H_2S-releasing moieties with the pharmacophore portion of rivastigmine, one of the few drugs currently used in AD therapy reported to be brain-selective.

As we recently reviewed, the main drawback in designing new clinically suitable H_2S-donor hybrids is to ensure a tissue specific and controlled cellular H_2S-release, avoiding systemic toxic effects. Therefore, in this work we initially aimed to validate the use of SFN and ERN as valuable H_2S releasing portions through the combination with the acetylcholinesterase inhibitor rivastigmine, to obtain new chemical entities able to target AD altered neuronal setting and microglia.

Then, we explored the pharmacological profile of this limited set of molecules in terms of anti-inflammatory and antioxidant activity, effects mainly related to the presence of H_2S releasing moiety, in order to validate the proof of concept of using ERN and SFN as natural occurring H_2S donor moieties for the design and synthesis of new H_2S-releasing drugs.

Since the induction of a pro-inflammatory state may correlate with grade of severity in neurodegeneration, we firstly investigated the H_2S-donor, anti-inflammatory, antioxidant and neuroprotective profile of our newly synthetized hybrids in microglia and neuronal cell lines. Results showed that both SFN- and ERN-derivatives show significant anti-inflammatory and antioxidant activities in microglia cell line, and induce the expression of proteins (i.e. GSH) involved in the antioxidant defense in neuronal cell line. In particular, all hybrids produced a significant decrease in ROS production elicited by pro-inflammatory stimulus compared to the native compound rivastigmine, which completely lacks of antioxidant activity. The new compounds were also able to reduce NO-release in microglia BV-2 cells whereas rivastigmine showed no effect. This result is mainly due to the multiple mechanisms of actions of SFN and ERN moieties and their capability to release H_2S. Moreover, the most active compounds 1 and 2 increased GSH level in neuronal SH-SY5Y cells. Notably, these two compounds present favorable logP values, suggesting their potential ability to reach the brain. In order to elucidate the mechanism of indirect antioxidant action at molecular level, we further explored the influence of compounds 1 and 2 on the activation of Nrf2 pathway in SH-SY5Y cells. While compound 2 showed a negligible activity, compound 1 exerted a time-dependent Nrf2 activation. We speculate that the lack of Nrf2 activation for compound 2 could be partially due to the high amount of gasotransmitter released inside the cells. Exogenous H_2S has been shown to have hormetic effects with antioxidant (involving Nrf2) and pro-oxidant activities at low and high concentrations, respectively [36,37].

In conclusion, we developed a set of original H_2S releasing hybrids starting from rivastigmine, a brain selective AchEI provided of a slight microglial neuroprotective capability against LPS-induced neuroinflammation, and SFN/ERN as natural-occurring H2S releasing moieties. Globally, our biological evaluation indicates compound 1 as a new well-balanced anti-inflammatory and antioxidant agent. This promising pharmacological profile could be partially due to the slow H_2S release and to the favorable logP, which promotes a cellular-specific activity.

Future *in vitro* investigation (i.e. permeability assay, AchE inhibition) will be of help in defining more in depth the pharmacological profile of compound 1 and will guide the *in vivo* evaluation in specific models of AD.

5. Experimental section

Chemistry. General Material and Methods. Melting points were determined on a Kofler hot-stage apparatus and are uncorrected. Chemical shifts (δ) are reported in parts per million downfield from

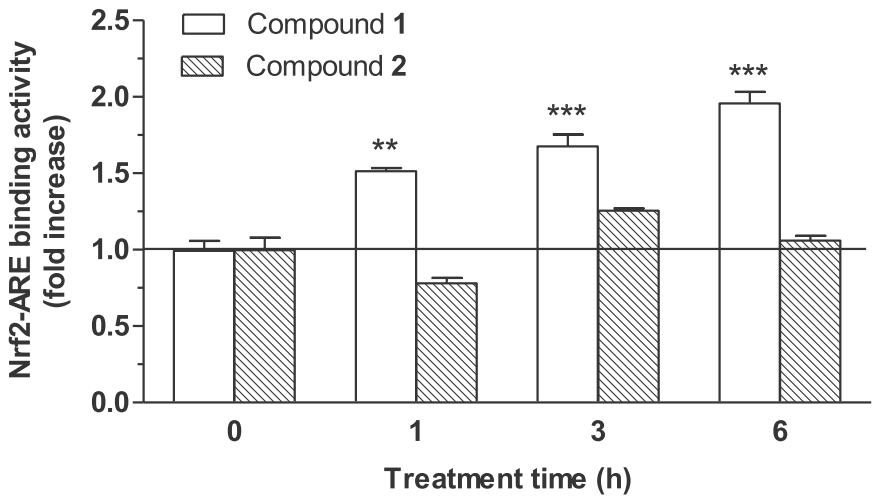

Fig. 8. Compound 1, but not compound 2, activates the Nrf2 protein in SH-SY5Y cells. Cells were incubated with compounds 1 and 2 (5 μM) for 1, 3 and 6 h. At the end of incubation, nuclear extraction and detection of active Nrf2 protein level were performed using the Nuclear Extract and TransAM Nrf2 Kit, respectively, as described in the Materials and Methods section. Data are expressed as fold increase and reported as mean ± SEM of three independent experiments (**$p < 0.01$ and ***$p < 0.001$ vs untreated cells at two-way ANOVA with Bonferroni post hoc test).

Table 1
Calculated logP per compounds 1–6 and their native drug rivastigmine. logP values were calculated by using the logP predictor plugin (Consensus Method) included in Marvin-Sketch 19.18 provided by ChemAxon.

Compound	Calculated logP
1	3,27
2	2,98
3	3,27
4	1,67
5	1,37
6	1,66
rivastigmine	2,41

tetramethylsilane and referenced from solvent references; coupling constants J are reported in hertz. 1H NMR and 13C NMR spectra of all compounds were obtained with a Bruker TopSpin 3.2400 MHz spectrometer. 13C NMR spectra were fully decoupled. The following abbreviations are used: singlet (s), doublet (d), triplet (t), double–doublet (dd), and multiplet (m). The elemental compositions of the compounds agreed to within ±0.4% of the calculated values. Chromatographic separation was performed on silica gel columns by flash (Kieselgel 40, 0.040–0.063 mm; Merck) or gravity column (Kieselgel 60, 0.063–0.200 mm; Merck) chromatography. HPLC purity determination was performed on a Varian Pro Star 330PDA detector, a binary HPLC pump Varian 9012 and a Rehodyne injector with 20 μl loop. A Thermos Scientific ™ Hypersil™ C18 ODS (5 μm, 250 × 4.6 mmID) HPLC column was used (detection at 220 nm). Chromatographic separation was carried out with a gradient of 20–80% acetonitrile in water (containing 0.1% TFA) over 20 min and a gradient of 80–20% over 10 min. Reactions were followed by thin-layer chromatography (TLC) on Merck aluminum silica gel (60 F254) sheets that were visualized under a UV lamp. Evaporation was performed *in vacuo* (rotating evaporator). Sodium sulfate was always used as the drying agent. Commercially available chemicals were purchased from Sigma-Aldrich or Alfa Aesar.

5.1. General procedure for the synthesis of isothiocyanates (1–3)

To a solution of amine 15–17 (0.10 mmol) in DCM (1 ml), under N_2 atmosphere and cooled to 0 °C, were added thiophosgene (0.03 ml, 0.32 mmol) and NaOH (10.9 mg, 0.27 mmol). The resulting suspension was stirred for 4 h at r.t. Then the solution was evaporated to dryness, rinsed with new DCM and filtered on Celite. The solution was dried and the crude product purified through flash chromatography.

5.1.1. 3-(2-((4-isothiocyanatobutyl)thio)acetamido)phenyl ethyl(methyl)carbamate (1)

Amine 15 (30.6 mg, 0.09 mmol) was reacted with thiophosgene (0.03 mL, 0.28 mmol) in the presence of NaOH (9.6 mg, 0.24 mmol). The crude product was purified through flash chromatography using PE/AcOEt 1:1 as eluting mixture to give derivative 1 (30.9 mg, 0.081 mmol, yield 90%). ^{1}H NMR ($CDCl_3$): δ 1.19 (t, $J = 7.0$ Hz, 1.5H, CH_3 rotamer); 1.22 (t, $J = 7.0$ Hz, 1.5H, CH_3 rotamer); 1.73–1.83 (m, 4H, CH_2); 2.63 (t, $J = 6.8$ Hz, 2H, CH_2S); 2.99 (s, 1.5H, CH_2 rotamer); 3.06 (s, 1.5H, CH_2 rotamer); 3.35 (s, 2H, CH_2CO); 3.40 (q, $J = 7.0$ Hz, 1H, CH_2 rotamer); 3.47 (q, $J = 7.0$ Hz, 1H, CH_2 rotamer); 3.54 (t, $J = 6.2$ Hz, 2H, CH_2N); 6.87–6.94 (m, 1H, Ar); 7.29–7.3 (m, 2H, Ar); 7.41–7.48 (m, 1H, Ar); 8.60 (br s, 1H, NH) ppm. ^{13}C NMR ($CDCl_3$): δ 167.08, 154.66, 151.98, 138.52, 129.64, 118.02, 117.95, 116.51, 113.67, 44.71, 44.24, 36.91, 34.39 (CH_2 rotamer), 33.97 (CH_2 rotamer), 32.16, 29.03, 26.12, 13.34 (CH_3 rotamer), 12.59 (CH_3 rotamer) ppm. HPLC purity: 97%.$t_R = 17.32$ min.

5.1.2. 3-((2-((4-isothiocyanatobutyl)thio)acetamido)methyl)phenyl ethyl(methyl)carbamate (2)

Amine 16 (35.4 mg, 0.10 mmol) was reacted with thiophosgene (0.03 mL, 0.32 mmol) in the presence of NaOH (10.9 mg, 0.27 mmol). The crude product was purified through flash chromatography using PE/AcOEt 1:1 as eluting mixture to give derivative 2 (11.9 mg, 0.03 mmol, 30% yield). ^{1}H NMR ($CDCl_3$): δ 1.19 (t, $J = 7.0$ Hz, 1.5H, CH_3 rotamer); 1.23 (t, $J = 7.0$ Hz, 1.5H, CH_3 rotamer); 1.65–1.77 (m, 4H, CH_2); 2.55 (t, $J = 7.8$ Hz, 2H, CH_2S); 2.98 (s, 1.5H, CH_3 rotamer); 3.06 (s, 1.5H, CH_3 rotamer); 3.26 (s, 2H, CH_2S); 3.41 (q, $J = 7.0$ Hz, 1H, CH_2 rotamer); 3.44–3.50 (m, 3H, CH_2 rotamer + CH_2NCS); 4.46 (d, $J = 6.0$ Hz, 2H, CH_2NH); 7.03–7.13 (m, 4H, Ar + NH); 7.31–7.35 (m, 1H, Ar) ppm. ^{13}C NMR ($CDCl_3$): δ 168.73, 154.58, 154.42, 151.97, 139.52, 129.74, 124.70, 121.47, 121.24, 44.68, 44.25, 43.62, 36.21, 34.39 (CH_2 rotamer), 33.97 (CH_2 rotamer), 32.26, 29.82, 29.00, 26.18, 13.37 (CH_3 rotamer), 12.59 (CH_3 rotamer) ppm. HPLC purity: 95%.$t_R = 22.06$ min.

5.1.3. 3-(2-(2-((4-isothiocyanatobutyl)thio)acetamido)ethyl)phenyl ethyl(methyl)carbamate (3)

Amine 17 (36.8 mg, 0.10 mmol) was reacted with thiophosgene (0.03 mL, 0.32 mmol) in the presence of NaOH (10.9 mg, 0.27 mmol). The crude product was purified through flash chromatography using PE/AcOEt 1:1 as eluting mixture to give derivative 3 (10.2 mg, 0.025 mmol, 25% yield). ^{1}H NMR ($CDCl_3$): δ 1.19 (t, $J = 7.2$ Hz, 1.5H, CH_3 rotamer); 1.25 (t, $J = 7.2$ Hz, 1.5H, CH_3 rotamer); 1.59–1.75 (m, 4H, CH_2CH_2); 2.43 (t, $J = 7.0$ Hz, 2H, CH_2S); 2.85 (t, $J = 6.8$ Hz, 2H, CH_2Ph); 2.98 (s, 1.5H, CH_3 rotamer); 3.06 (s, 1.5H, CH_3 rotamer); 3.16 (s, 2H, CH2S); 3.41 (q, $J = 7.2$ Hz, 1H, CH_2 rotamer); 3.46–3.51 (m, 3H, CH_2 rotamer + CH_2NCS); 3.57 (q, $J = 6.4$ Hz, 2H, CH_2NH); 6.80 (br s, 1H, NH); 6.98–7.04 (m, 3H, Ar); 7.27–7.31 (m, 1H, Ar) ppm. ^{13}C NMR ($CDCl_3$): δ 168.75, 154.65, 154.49, 151.92, 140.16, 129.53, 125.60, 122.33, 120.15, 44.71 (CH_3 rotamer), 44.23 (CH_3 rotamer), 40.56, 36.10, 35.28, 34.38 (CH_2 rotamer), 33.96 (CH_2 rotamer), 32.05, 29.81, 28.96, 26.10, 13.37 (CH_3 rotamer), 12.60 (CH_3 rotamer) ppm. HPLC purity: 95%.$t_R = 18.07$ min.

5.2. General procedure for the synthesis of isothiocyanates (4–6)

A solution of Oxone® (43.0 mg, 0.07 mmol) in H_2O (0.33 ml) was added to isothiocyanates 1–3 (0.12 mmol) dissolved in CH_3OH/THF (1:1, 0.70 ml) and cooled to 0 °C. The reaction mixture was stirred for 1 h at r.t. Then the organic solvent was evaporated and the residue aqueous phase extracted several times with AcOEt. Then the organic layer was washed with brine, dried over anhydrous Na_2SO_4 and evaporated to dryness.

5.2.1. 3-(2-((4-isothiocyanatobutyl)sulfinyl)acetamido)phenyl ethyl(methyl)carbamate (4)

Compound 4 (9.1 mg, 0.023 mmol, 46% yield) was obtained from isothiocyanate 1 (19.1 mg, 0.05 mmol) through oxidation with Oxone® (19.4 mg, 0.03 mmol). The crude product was purified through flash chromatography using a gradient of PE/AcOEt (from 7:3 to 0:10) as the eluent. ^{1}H NMR ($CDCl_3$): δ 1.22 (t, $J = 7.2$, 1.5H, CH_3 rotamer); 1.27 (t, $J = 7.0$ Hz, 1.5H, CH_3 rotamer); 1.85–1.99 (m, 4H, CH_2); 2.89–2.98 (m, 2H, CH_2SO); 3.01 (s, 1.5H, CH2 rotamer); 3.09 (s, 1.5H, CH2 rotamer); 3.43 (q, $J = 7.2$ Hz, 1H, CH_2 rotamer); 3.48 (q, $J = 7.0$ Hz, 1H, CH_2 rotamer); 3.51 (d, $J = 14$ Hz, 1H, CH_2CO); 3.61 (t, $J = 6.0$ Hz, 2H, CH_2N); 3.84 (d, $J = 14$ Hz, 1H, CH_2CO); 6.83–6.92 (m, 1H, Ar); 7.21–7.30 (m, 2H, Ar); 7.42–7.49 (m, 1H, Ar); 9.19 (br s, 1H, NH) ppm. ^{13}C NMR ($CDCl_3$): δ: 162.05, 151.97, 152, 138.35, 131.45, 129.65, 118.35, 117.06, 114.18, 54.10, 50.66, 44.70 (CH_3 rotamer), 44.25 (CH_3 rotamer), 39.99 (CH_2 rotamer), 39.10, 34.42 (CH_2 rotamer), 29.82, 29.09, 13.35 (CH_3 rotamer), 12.60 (CH_3 rotamer) ppm. HPLC purity: 95%.$t_R = 20.02$ min.

5.2.2. 3-((2-((4-isothiocyanatobutyl)sulfinyl)acetamido)methyl) phenyl ethyl(methyl)carbamate (5)

Compound 5 (11.9 mg, 0.029 mmol, 24% yield) was obtained from isothiocyanate 2 (47.5 mg, 0.12 mmol) through oxidation with Oxone® (43.0 mg, 0.07 mmol). The crude product was purified through flash chromatography using a gradient of PE/AcOEt (from 9:1 to 0:10) as the eluent. ^{1}H NMR ($CDCl_3$): δ 1.20 (t, $J = 7.2$ Hz, 1.5H, CH_3 rotamer); 1.24 (t, $J = 7.2$ Hz, 1.5H, CH_3 rotamer); 1.79–1.88 (m, 4H, CH_2); 2.70–2.77 (m, 1H, CH_2SO); 2.81–2.87 (m, 1H, CH_2SO); 2.98 (s, 1.5H, CH_3 rotamer); 3.06 (s, 1.5H, CH_3 rotamer); 3.30 (d, $J = 14.2$ Hz, 1H, CH_2SO); 3.40 (q, $J = 7.2$ Hz, 1H, CH_2 rotamer); 3.45 (q, $J = 7.2$ Hz, 1H, CH_2 rotamer); 3.54 (t, $J = 5.8$ Hz, 2H, CH_2NCS); 3.71 (d, $J = 14.2$ Hz, 1H, CH_2SO); 4.39–4.44 (m, 1H, CH_2Ph); 4.52–4.57 (m, 1H, CH_2Ph); 7.02–7.16 (m, 3H, Ar); 7.30–7.34 (m, 1H, Ar) ppm. ^{13}C NMR ($CDCl_3$): δ 163.84, 154.63, 154.47, 151.89, 139.30, 129.65, 124.87, 121.60, 121.22, 54.39, 50.56, 44.63, 44.24, 43.55, 34.37 (CH_2 rotamer), 33.96 (CH_2 rotamer), 29.00, 20.37, 13.35 (CH_3 rotamer), 12.58 (CH_3 rotamer) ppm. HPLC purity: 96%.$t_R = 16.51$ min.

5.2.3. 3-(2-(2-((4-isothiocyanatobutyl)sulfinyl)acetamido)ethyl) phenyl ethyl(methyl)carbamate (6)

Compound 6 (17.0 mg, 0.04 mmol, 33% yield) was obtained from isothiocyanate 3 (49.1 mg, 0.12 mmol) through oxidation with Oxone® (43.0 mg, 0.07 mmol). The crude product was purified through flash chromatography using AcOEt as the eluent. ^{1}H NMR ($CDCl_3$): δ 1.20 (t, $J = 7.2$ Hz, 1.5H, CH_3 rotamer); 1.25 (t, $J = 7.2$ Hz, 1.5H, CH_3 rotamer); 1.79–1.89 (m, 4H, CH_2CH_2); 2.71–2.82 (m, 2H, CH_2S); 2.86 (t, $J = 7.4$ Hz, 2H, CH_2Ph); 2.97 (s, 1.5H, CH_3 rotamer); 3.06 (s, 1.5H, CH_3 rotamer); 3.30 (d, $J = 14.0$ Hz, 1H, CH_2SO); 3.41 (q, $J = 7.2$ Hz, 1H, CH_2 rotamer); 3.50 (q, $J = 7.2$ Hz, 1H, CH_2 rotamer); 3.56–3.60 (m, 4H, CH_2NH + CH_2NCS); 3.61 (d, $J = 14.0$ Hz, 1H, CH_2SO); 6.96–7.00 (m, 3H, Ar + br NH); 7.04 (d, $J = 7.6$ Hz, 1H, Ar); 7.28–7.30 (m, 1H, Ar) ppm. ^{13}C NMR ($CDCl_3$): δ 163.87, 154.75, 151.76, 140.07, 131.22, 129.50, 125.72, 122.44, 120.09, 54.47, 50.67, 44.66, 44.22, 40.69, 35.27, 34.37 (CH_2 rotamer), 33.94 (CH_2 rotamer), 29.01, 20.37, 13.34 (CH_3 rotamer), 12.58 (CH_3 rotamer) ppm. HPLC purity: 97%.$t_R = 17.05$ min.

5.3. General procedure for the synthesis of derivatives (12–15)

To a solution of thiol 10 (232.9 mg, 0.99 mmol) and KOH (111 mg, 1.99 mmol) in acetone (5 mL) was added the appropriate chloroderivative 11a-c (0.99 mmol) [13]. The resulting mixture was refluxed for 12 h, then the solid was filtered off and the solution evaporated to dryness.

5.3.1. 3-(2-((4-(1,3-dioxoisoindolin-2-yl)butyl)thio)acetamido) phenyl ethyl(methyl)carbamate (12)

Carbamate 12 (122 mg, 0.26 mmol, 26% yield) was synthetized starting from thiol 10 (232.9 mg, 0.99 mmol) and chloroderivative 11a (268.0 mg 0.99 mmol). The crude product was purified by flash chromatography using PE/AcOEt (1:1) as eluting mixture. ^{1}H NMR ($CDCl_3$): δ 1.18 (t, $J = 7.2$ Hz, 1.5H, CH_3 rotamer); 1.25 (t, $J = 7.2$ Hz, 1.5H, CH_3 rotamer); 1.65–1.71 (m, 2H, CH_2); 1.76–1.81 (m, 2H, CH_2); 2.64 (t, $J = 7.4$ Hz, 2H, CH_2S); 2.97 (s, 1.5H, CH_2 rotamer); 3.06 (s, 1.5H, CH_2 rotamer); 3.33 (s, 2H, CH_2CO); 3.36 (q, $J = 6.8$ Hz, 1H, CH_2 rotamer); 3.44 (q, $J = 6.8$ Hz, 1H, CH_2 rotamer); 3.70 (t, $J = 7.0$ Hz, 2H. CH_2N); 6.86–6.94 (m, 1H, Ar); 7.27–7.34 (m, 2H, Ar); 7.44–7.49 (m, 1H, Ar); 7.70–7.72 (m, 2H, Ar); 7.81–7.87 (m, 2H, Ar); 8.74 (br s, 1H, NH) ppm.

5.3.2. 3-((2-((4-(1,3-dioxoisoindolin-2-yl)butyl)thio)acetamido) methyl)phenylethyl(methyl)carbamate (13)

Carbamate 13 (193.4 mg, 0.4 mmol, 40% yield) was synthetized starting from thiol 10 (232.9 mg, 0.99 mmol) and chloroderivative 11b (281.9 mg, 0.99 mmol). The crude product was purified by flash chromatography using PE/AcOEt (7:3) as eluting mixture. ^{1}H NMR ($CDCl_3$): δ 1.16 (t, $J = 7.2$ Hz, 1.5H, CH_3 rotamer); 1.20 (t, $J = 7.2$ Hz, 1.5H, CH_3 rotamer); 1.59–1.63 (m, 2H, CH_2); 1.70–1.76 (m, 2H, CH_2); 2.57 (t, $J = 7.2$ Hz, 2H, CH_2S); 2.96 (s, 1.5H, CH_3 rotamer); 3.04 (s, 1.5H, CH_3 rotamer); 3.25 (s, 2H, CH_2S); 3.39 (q, $J = 7.2$ Hz, 1H, CH_2 rotamer); 3.44 (q, $J = 7.2$ Hz, 1H, CH_2 rotamer); 3.64 (t, $J = 7.0$ Hz, 2H, CH_2N); 4.47 (d, $J = 6.0$ Hz, 2H, CH_2NH); 7.00–7.04 (m, 2H, Ar); 7.11 (d, $J = 7.6$ Hz, 1H, Ar); 7.28–7.32 (m, 1H, Ar); 7.68–7.73 (m, 2H, Ar); 7.80–7.84 (m, 2H, Ar) ppm.

5.3.3. 3-(2-(2-((4-(1,3-dioxoisoindolin-2-yl)butyl)thio)acetamido) ethyl)phenylethyl(methyl)carbamate (14)

Carbamate 14 was synthetized starting from thiol 10 (232.9 mg, 0.99 mmol) and chloroderivative 11c (295.8 mg, 0.99 mmol). The crude product was purified by flash chromatography using AcOEt as

the eluent (238.6 mg, 0.48 mmol, 48% yield). ^{1}H NMR ($CDCl_3$): δ 1.16 (t, $J = 7.2$ Hz, 1.5H, CH_3 rotamer); 1.22 (t, $J = 7.2$ Hz, 1.5H, CH_3 rotamer); 1.50–1.58 (m, 2H, CH_2); 1.66–1.74 (m, 2H, CH_2); 2.45 (t, $J = 7.4$ Hz, 2H, CH_2S); 2.81 (t, $J = 7.0$ Hz, 2H, CH_2Ph); 2.94 (s, 1.5H, CH_3 rotamer); 3.02 (s, 1.5H, CH_3 rotamer); 3.13 (s, 2H, CH_2S); 3.37 (q, $J = 7.2$ Hz, 1H, CH_2 rotamer); 3.41 (q, $J = 7.2$ Hz, 1H, CH_2 rotamer); 3.52 (q, $J = 7.0$ Hz, 2H, CH_2NH); 3.62 (t, $J = 7.0$ Hz, 2H, CH_2N); 6.95–7.00 (m, 3H, Ar); 7.22–7.26 (m, 1H, Ar); 7.67–7.69 (m, 2H, Ar); 7.79–7.81 (m, 2H, Ar) ppm.

5.4. General procedure for the synthesis of derivatives (15–17)

To a solution of the opportune derivative 12–14 (0.22 mmol) in MeOH (1.3 ml) was added hydrazine monohydrate (0.54 mmol, 0.03 ml); the resulting mixture was refluxed for 4 h. Once verified the disappearance of starting material by TLC, the solution was cooled, diluted with AcOEt and washed with NaOH 1 N. The organic layer was then dried over Na_2SO_4 and evaporated to dryness.

5.4.1. 3-(2-((4-aminobutyl)thio)acetamido)phenyl ethyl(methyl) carbamate (15)

Amine 15 (44.1 mg, 0.13 mmol, 75% yield) was obtained starting from derivative 12 (79.8 mg, 0.17 mmol). ^{1}H NMR ($CDCl_3$): δ 1.18 (t, $J = 7.0$ Hz, 1.5H, CH_3 rotamer); 1.25 (t, $J = 7.0$ Hz, 1.5H, CH_3 rotamer); 1.65–1.71 (m, 4H, CH_2); 2.58 (t, $J = 6.4$ Hz, 2H, CH_2S); 2.70–2.78 (m, 2H, NH_2); 2.97 (s, 1.5H, CH_2 rotamer); 3.06 (s, 1.5H, CH_2 rotamer); 3.39 (s, 2H, CH_2CO); 3.48 (q, $J = 6.8$ Hz, 1H, CH_2 rotamer); 3.48 (q, $J = 6.4$ Hz, 1H, CH_2 rotamer); 6.80–6.91 (m, 1H, Ar); 7.28–7.31 (m, 1H, Ar); 7.40–7.48 (m, 2H, Ar); 9.30 (br s, 1H, NH) ppm.

5.4.2. 3-((2-((4-aminobutyl)thio)acetamido)methyl)phenyl ethyl(methyl)carbamate (16)

Amine 16 (60.0 mg, 0.17 mmol, 75% yield) was obtained starting from derivative 13 (106.4 mg, 0.22 mmol). ^{1}H NMR ($CDCl_3$): δ 1.18 (t, $J = 7.0$ Hz, 1.5H, CH_3 rotamer); 1.23 (t, $J = 7.0$ Hz, 1.5H, CH_3 rotamer); 1.46–1.56 (m, 2H, CH_2); 1.58–1.62 (m, 2H, CH_2); 2.52 (t, $J = 7.4$ Hz, 2H, CH_2S); 2.64 (t, $J = 6.8$ Hz, 2H, CH_2NH_2); 2.97 (s, 1.5H, CH_3 rotamer); 3.06 (s, 1.5H, CH_3 rotamer); 3.26 (s, 2H, CH_2S); 3.39 (q, $J = 7.0$ Hz, 1H, CH_2 rotamer); 3.46 (q, $J = 7.0$ Hz, 1H, CH_2 rotamer); 4.46 (d, $J = 6.0$ Hz, 2H, CH_2NH); 7.02–7.05 (m, 2H, Ar); 7.12 (d, $J = 7.6$ Hz, 1H, Ar); 7.30–7.34 (m, 2H, Ar + NH) ppm.

5.4.3. 3-(2-(2-((4-aminobutyl)thio)acetamido)ethyl)phenyl ethyl(methyl)carbamate (17)

Amine 17 (77.2 mg, 0.21 mmol, 95% yield) was obtained starting from derivative 14 (109.4 mg, 0.22 mmol). ^{1}H NMR ($CDCl_3$): δ 1.20 (t, $J = 7.2$ Hz, 1.5H, CH_3 rotamer); 1.25 (t, $J = 7.2$ Hz, 1.5H, CH_3 rotamer); 1.43–1.47 (m, 2H, CH_2); 1.48–1.60 (m, 2H, CH_2); 2.43 (t, $J = 7.2$ Hz, 2H, CH_2S); 2.67 (t, $J = 6.8$ Hz, 2H, CH_2NH_2); 2.85 (t, $J = 7.0$ Hz, 2H, CH_2Ph); 2.98 (s, 1.5H, CH_3 rotamer); 3.06 (s, 1.5H, CH_3 rotamer); 3.18 (s, 2H, CH_2S); 3.42 (q, $J = 7.2$ Hz, 1H, CH_2 rotamer); 3.46 (q, $J = 7.2$ Hz, 1H, CH_2 rotamer); 3.56 (q, $J = 6.8$ Hz, 2H, CH_2NH); 6.93 (br s, 1H, NH); 6.98–7.04 (m, 3H, Ar); 7.27–7.31 (m, 1H, Ar) ppm.

5.4.4. 2-(4-bromobutyl)isoindoline-1,3-dione (8)

Potassium phthalimide salt 7 (572 mg, 3.09 mmol) was added to a solution of 1,4-dibromobutane (2.0 g, 1.11 ml, 9.26 mmol) in acetone (5 mL). The reaction mixture was refluxed for 12 h; later the solid was filtered off and the resulting solution was evaporated under reduced pressure. The crude product was purified through flash chromatography using EP/AcOEt 9:1 as eluting mixture to afford derivative 8 (696.9 mg, 2.47 mmol, 80% yield). ^{1}H NMR ($CDCl_3$): δ 1.83–1.93 (m, 4H, CH_2); 3.44 (t, $J = 6.4$ Hz, 2H, CH_2Br); 3.72 (t, $J = 6.8$ Hz, 2H, CH_2N); 7.71–7.73 (m, 2H, Ar); 7.83–7.86 (m, 2H, Ar) ppm.

5.4.5. S-(4-(1,3-dioxoisoindolin-2-yl)butyl) ethanethioate (9)

Bromoderivative 8 (601.0 mg, 2.13 mmol) dissolved in THF (26 mL) was reacted with potassium thioacetate (729 mg, 6.38 mmol). The mixture was refluxed for 12 h, then cooled and evaporated under vacuum. The crude residue was diluted with H_2O and extracted with AcOEt; the organic layer was then washed several times with brine, dried over anhydrous Na_2SO_4 and evaporated to dryness to provide the desired product 9 (479 mg, 1.73 mmol 81% yield). ^{1}H NMR ($CDCl_3$): δ 1.61–1.66 (m, 2H, CH_2); 1.71–1.79 (m, 2H, CH_2); 2.31 (s, 3H, CH_3); 2.90 (t, $J = 7.2$ Hz, 2H, CH_2S); 3.69 (t, $J = 7.0$ Hz, 2H, CH_2N); 7.70–7.72 (m, 2H, Ar); 7.83–7.85 (m, 2H, Ar) ppm.

5.4.6. 2-(4-mercaptobutyl)isoindoline-1,3-dione (10)

To a solution of compound 9 (496 mg, 1,79 mmol) in dry MeOH (5.37 mL), under N_2 atmosphere, was added HCl 37% (0.72 mL). The resulting solution was refluxed for 5 h, then diluted with H_2O and extracted with AcOEt. Finally, the organic layer dried over anhydrous Na_2SO_4 and evaporated to dryness to provide the desired product 10 (371 mg, 1.58 mmol 88% yield). ^{1}H NMR ($CDCl_3$): δ 1.35 (t, $J = 7.5$ Hz, 1H, SH); 1.64–1.70 (m, 2H, CH_2); 1.76–1.84 (m, 2H, CH_2); 2.57 (q, $J = 7.5$ Hz, 2H, CH_2S); 3.70 (t, $J = 7.0$ Hz, 2H, CH_2N); 7.70–7.72 (m, 2H, Ar); 7.83–7.85 (m, 2H, Ar) ppm.

5.5. Cell culture

The immortalized murine microglial cell line BV-2 (IRCCS Ospedale Policlinico San Martino-IST Istituto Nazionale per la Ricerca sul Cancro, Genova, Italy) was cultured in RPMI 1640 (Sigma-Aldrich) supplemented with 2 mM Glutamine (Sigma-Aldrich), 5% Fetal Bovine Serum (FBS) (Sigma-Aldrich) and 1% of 100 units/ml penicillin and 100 mg/ml streptomycin (Sigma Aldrich) in tissue culture flasks at 37 °C in a humidified atmosphere and 5% CO_2.

Human neuronal (SH-SY5Y) cells were routinely grown in Dulbecco's modified Eagle's Medium supplemented with 10% fetal bovine serum, 2 mM L-glutamine, 50 U/mL penicillin and 50 μg/mL streptomycin at 37 °C in a humidified incubator with 5% CO_2.

5.6. Evaluation of H_2S release on BV-2

The evaluation of H_2S release into the cytosol of BV-2 was assessed by spectrofluorometric method as already described [33,38]. Briefly, BV-2 were cultured up to about 90% confluence. 24 h before the experiment, cells were seeded onto a 96-well black plate, at density of 72×10^3 per well in serum free medium. After 24 h the cells were pre-loaded with a 100 μM solution of the fluorescent dye WSP-1 (Washington State Probe-1, Cayman Chemical). In particular, WSP-1 was first incubated with BV-2 for 30 min (allowing cells to up-load the dye), then the supernatant was removed and replaced with a solution of the tested compounds (1–6), reference drug or vehicle (dimethyl sulfoxide, DMSO 1%). The tested compounds (100 μM) and the reference drug diallyl disulfide (DADS) 100 μM [39], were first dissolved in DMSO and then diluted in buffer standard (HEPES 20 mM, NaCl 120 mM, KCl 2 mM, $CaCl_2 \cdot 2H_2O$ 2 mM, $MgCl_2 \cdot 6H_2O$ 1 mM, Glucose 5 mM, pH 7.4, at room temperature). When WSP-1 reacts with H_2S, it releases a fluorophore detectable by a spectrofluorometer at $\lambda = 465–515$ nm. The increase of the fluorescence index (FI) was monitored for 45 min, through a spectrofluorometer (EnSpire, PerkinElmer) and expressed as the area under the curve (AUC).

5.7. Analysis of cell viability, ROS and nitric oxide (NOx)

5.7.1. General conditions

BV-2 were seeded onto 6 well plates in serum free medium at a density per well of 5×10^5 and after 24 h, the cells were treated with the tested compounds (1–6) at the concentration of 1 μM, with rivastigmine 1 μM or with vehicle (DMSO 0.1%). After 1 h, cells were stimulated with lipopolysaccharide 5 μg/mL (LPS, Sigma-Aldrich, O111:B4 *E. coli*) for 24 h. Cell viability, ROS and NOx were assessed as follow with the Muse Cell Analyzer: cells were detached, centrifuged for 5 min 1100 rpm and resuspended at the density of 1×10^6 to 1×10^7 cells/ml in the provided 1X Assay Buffer.

5.7.2. Cell viability

20 μL of the cell suspension (prepared as previously described: see general conditions) were added to 380 μL of Muse™ Count & Viability Reagent and incubated protected from light at room temperature for 5 min. Each sample was analyzed by the Muse™ Cell Analyzer using "Count and Cell Viability" protocol. Data are expressed as percentage of cell viability recorded for BV-2 cells treated with vehicle.

5.7.3. ROS

The Muse® Oxidative Stress Reagent working solution for cell staining has been prepared immediately before use by diluting Muse® Oxidative Stress Reagent stock solution 1:8000 in 1X Assay Buffer following the manufacture's instruction. 10 μL of the cell suspension (see general conditions) were added to 190 μL of Muse® Oxidative Stress Reagent working solution and incubated protected from light at 37 °C for 30 min. Each sample was analyzed by the Muse™ Cell Analyzer using "Oxidative stress" protocol. Data are expressed as percentage of ROS recorded for BV-2 cells treated with vehicle.

5.7.4. Nitric oxide

The Muse® Nitric Oxide working solution was prepared immediately before use by diluting the Muse® Nitric Oxide Reagent stock solution 1:1000 in 1X Assay Buffer, while the Muse® 7-AAD working solution was obtained by diluting the Muse® 7-AAD stock solution 1:45 in 1X Assay Buffer (see manufacturer's instructions). 10 μL of cell suspension (see general conditions) were added to 100 μL of Muse® Nitric Oxide Reagent working solution and each sample was incubated for 30 min in the 37 °C incubator with 5% CO_2. Then, 90 μL of Muse® 7-AAD working solution were added to each sample and incubate at room temperature for 5 min, protected from light. Then, samples were analyzed by the Muse™ Cell Analyzer using "Nitric Oxide" protocol. Data are expressed as percentage of NOx recorded for BV-2 cells treated with vehicle.

5.7.5. Statistical analysis

Experiments were performed in triplicate each in three replicates. All data are expressed as mean ± standard error (SEM); Student *t*-test (followed by Bonferroni post hoc test, when required) was selected as statistical analysis, $p < 0.05$ was considered representative of significant statistical differences (software: GraphPad Prism 6.0).

5.7.6. Determination of neuronal viability

To establish the range of concentrations not associated with neurotoxicity, SH-SY5Y cells were seeded in a 96-well plate at 2×10^4 cells/well, incubated for 24 h and subsequently incubated with different concentrations of the hybrid compounds 1, 2 and 4–6 (1.25–40 μM) for 24 h at 37 °C in 5% CO_2. The neuronal viability, in terms of mitochondrial metabolic function, was evaluated by the reduction of 3-(4,5-dimethyl-2-thiazolyl)-2,5-diphenyl-2H-tetrazolium bromide (MTT) to its insoluble formazan, as previously described [40]. Briefly, the treatment medium was replaced with MTT in Hank's Balanced Salt Solution (HBSS) (0.5 mg/mL) for 2 h at 37 °C in 5% CO_2. After washing with HBSS, formazan crystals were dissolved in isopropanol. The amount of formazan was measured (570 nm, reference filter 690 nm) using the multilabel plate reader VICTOR™ X3 (PerkinElmer, Waltham, MA, USA). The quantity of formazan was directly proportional to the number of viable cells. Data are expressed as percentage of neuronal viability versus untreated cells.

5.7.7. Determination of antioxidant activity

The intracellular antioxidant activity of the studied compounds was evaluated in SH-SY5Y cells as previously described [41]. Briefly, cells were seeded in a 96-well plate at 2×10^4 cells/well, incubated for 24 h and subsequently incubated with the hybrid compounds 1, 2 and 4–6 (5 μM) for 24 h at 37 °C in 5% CO_2. At the end of incubation, the treatment medium was removed and 100 μL of a fluorescent probe, 2′–7′ dichlorodihydrofluorescein diacetate (DCFH-DA) (10 μg/mL), was added to each well. After 30 min of incubation at room temperature, DCFH-DA solution was replaced with a solution of hydrogen peroxide (H_2O_2) (50 μM) or *tert*-butyl hydroperoxide (*t*-BuOOH) (50 μM) for 30 min. The reactive oxygen species (ROS) formation was measured (excitation at 485 nm and emission at 535 nm) using the multilabel plate reader VICTOR™ X3 (PerkinElmer). The antioxidant activity is expressed as inhibition percentage of ROS formation induced by H_2O_2 or *t*-BuOOH.

5.7.8. Determination of glutathione levels

The glutathione (GSH) levels were evaluated in SH-SY5Y cells as previously described [42]. Briefly, cells were seeded in a black 96-well plate at 2×10^4 cells/well, incubated for 24 h and subsequently incubated with the hybrid compounds 1, 2 and 4–6 (5 μM) for 24 h at 37 °C in 5% CO_2. At the end of incubation, the treatment medium was removed and 100 μL of a fluorescent probe, monochlorobimane (MCB), was added to each well. After 30 min of incubation at 37 °C in 5% CO_2, the GSH levels were measured (excitation at 355 nm and emission at 460 nm) using the multilabel plate reader VICTOR™ X3 (PerkinElmer). Data are expressed as increase percentage of GSH levels.

5.7.9. Nuclear extraction and determination of active Nrf2 protein level

SH-SY5Y cells were seeded in 100 mm dishes at 2×10^6 cells/dish and incubated with the hybrid compounds 1 and 2 (5 μM) for 1, 3 and 6 h at 37 °C in 5% CO_2. At the end of incubation, nuclear extraction and determination of active Nrf2 protein level were performed using the Nuclear Extract and TransAM Nrf2 Kit (Active Motif, Carlsbad, CA, USA), respectively, according to the manufacturer's guidelines. The TransAM Nrf2 Kit is a DNA-binding ELISA able to determine the active Nrf2 protein level in nuclear extract. The primary antibody of the kit is able to recognize an epitope on Nrf2 protein upon ARE binding. The active Nrf2 protein levels in the treated cells are expressed as fold increase with respect to corresponding untreated cells.

5.7.10. $A\beta_{1-42}$ oligomers preparation

$A\beta_{1-42}$ peptide was first dissolved in 1,1,1,3,3,3-hexafluoroisopropanol to 1 mg/mL, sonicated, incubated at room temperature for 24 h and lyophilized. The resulting unaggregated $A\beta_{1-42}$ peptide film was dissolved with dimethyl sulfoxide and stored at −20 °C until use. The $A\beta_{1-42}$ peptide aggregation to oligomeric form was prepared as previously described [43].

5.7.11. MTT formazan exocytosis assay

The neuroprotection of the studied compounds against $A\beta_{1-42}$ was evaluated in SH-SY5Y cells as previously described [44]. Cells were seeded in a 96-well plate at 3×10^4 cells/well, incubated for 24 h and subsequently incubated with the hybrid compounds 1, 2 and 4–6 (5 μM) for 24 h and then with $A\beta_{1-42}$ oligomers (10 μM) for 4 h at 37 °C in 5% CO_2. The neuroprotective activity, in terms of increase in intracellular MTT granules, was measured by MTT formazan exocytosis assay. Briefly, the treatment medium was replaced with MTT in HBSS (0.5 mg/mL) for 1 h at 37 °C in 5% CO_2. After the incubation, intracellular MTT granules were completely solubilized in Tween-20 (10% v/v). The absorbance of Tween-20 soluble MTT was measured at 570 nm (reference filter 690 nm) using the multilabel plate reader VICTOR™ X3 (PerkinElmer). Data are expressed as percentage of neurotoxicity.

Funding sources

This work was supported by grant from International Society of Drug Discovery (ISDD), Milan and from the University of Pisa Progetto di Ricerca di Ateneo 2018 (PRA_2018_20 to SR).

Acknowledgements

The authors thank the COST action CA15135 (Multitarget Paradigm for Innovative Ligand Identification in the Drug Discovery Process MuTaLig) for support. They also thank POR FSE 2014–2020 – Regione Toscana and the University of Pisa for financing the fellowship to SS.

Appendix. ASupplementary data

Supplementary data related to this article can be found at https://doi.org/10.1016/j.ejmech.2019.111745.

References

[1] S. Sestito, G. Nesi, R. Pi, M. Macchia, S. Rapposelli, Hydrogen sulfide: a worthwhile tool in the design of new multitarget drugs, Front. Chem. 5 (2017) 72.
[2] Z.-Z. Xie, Y. Liu, J.-S. Bian, Hydrogen Sulfide and Cellular Redox Homeostasis, Oxidative Med. Cell. Longev. 2016 (2016), 6043038.
[3] R.C. Zanardo, V. Brancaleone, E. Distrutti, S. Fiorucci, G. Cirino, J.L. Wallace, R.C. Zanardo, V. Brancaleone, E. Distrutti, S. Fiorucci, Hydrogen sulfide is an endogenous modulator of leukocyte mediated inflammation, FASEB J. 20 (2006) 2118–2120.
[4] D. Wu, H. Wang, T. Teng, S. Duan, A. Ji, Y. Li, Hydrogen sulfide and autophagy: a double edged sword, Pharmacol. Res. 131 (2018) 120–127.
[5] W.-L. Chen, Y.-Y. Niu, W.-Z. Jiang, H.-L. Tang, C. Zhang, Q.-M. Xia, X.-Q. Tang, Neuroprotective effects of hydrogen sulfide and the underlying signaling pathways, Rev. Neurosci. 26 (2015) 129–142.
[6] B. Qabazard, L. Li, J. Gruber, M.T. Peh, L.F. Ng, S.D. Kumar, P. Rose, C.H. Tan, B.W. Dymock, F. Wei, S.C. Swain, B. Halliwell, S.R. Sturzenbaum, P.K. Moore, Hydrogen sulfide is an endogenous regulator of aging in Caenorhabditis elegans, Antioxidants Redox Signal. 20 (2014) 2621–2630.
[7] D.L. Miller, M.B. Roth, Hydrogen sulfide increases thermotolerance and lifespan in Caenorhabditis elegans, in: Proceedings of the National Academy of Sciences of the United States of America 104, 2007, pp. 20618–20622.
[8] P. Michalska, I. Buendia, L. Del Barrio, R. Leon, Novel multitarget hybrid compounds for the treatment of Alzheimer's disease, Curr. Top. Med. Chem. 17 (2017) 1027–1043.
[9] M.J. Oset-Gasque, J. Marco-Contelles, Alzheimer's disease, the "One-Molecule, one-target" paradigm, and the multitarget directed Ligand, Approach 9 (2018) 401–403.
[10] G. Nesi, S. Sestito, M. Digiacomo, S. Rapposelli, Oxidative stress, mitochondrial abnormalities and proteins deposition: multitarget approaches in Alzheimer's disease, Curr. Top. Med. Chem. (2017).
[11] Z. Chen, M. Digiacomo, Y. Tu, Q. Gu, S. Wang, X. Yang, J. Chu, Q. Chen, Y. Han, J. Chen, G. Nesi, S. Sestito, M. Macchia, S. Rapposelli, R. Pi, Discovery of novel rivastigmine-hydroxycinnamic acid hybrids as multi-targeted agents for Alzheimer's disease, Eur. J. Med. Chem. 125 (2017) 784–792.
[12] G. Nesi, Q. Chen, S. Sestito, M. Digiacomo, X. Yang, S. Wang, R. Pi, S. Rapposelli, Nature-based molecules combined with rivastigmine: a symbiotic approach for the synthesis of new agents against Alzheimer's disease, Eur. J. Med. Chem. 141 (2017) 232–239.
[13] S. Sestito, S. Wang, Q. Chen, J. Lu, S. Bertini, C. Pomelli, G. Chiellini, X. He, R. Pi, S. Rapposelli, Multi-targeted ChEI-copper chelating molecules as neuroprotective agents, Eur. J. Med. Chem. 174 (2019) 216–225.
[14] S. Sestito, S. Daniele, D. Pietrobono, V. Citi, L. Bellusci, G. Chiellini, V. Calderone, C. Martini, S. Rapposelli, Memantine prodrug as a new agent for Alzheimer's Disease, Sci. Rep. 9 (2019) 4612.
[15] R.J. Polinsky, Clinical pharmacology of rivastigmine: a new-generation acetylcholinesterase inhibitor for the treatment of Alzheimer's disease, Clin. Ther. 20 (1998) 634–647.
[16] C. Kala, S.S. Ali, N. Ahmad, S.J. Gilani, N. Ali Khan, Isothiocyanates: a review, Res J Pharmacogn 5 (2018) 71–89.
[17] A. Sunkaria, S. Bhardwaj, A. Yadav, A. Halder, R. Sandhir, Sulforaphane attenuates postnatal proteasome inhibition and improves spatial learning in adult mice, J. Nutr. Biochem. 51 (2018) 69–79.
[18] M.S. Jaafaru, N.A. Abd Karim, M.E. Enas, P. Rollin, E. Mazzon, Protective Effect of Glucosinolates Hydrolytic Products in Neurodegenerative Diseases, NDDs), 2018, p. 10.
[19] A. Tarozzi, F. Morroni, A. Merlicco, S. Hrelia, C. Angeloni, G. Cantelli-Forti, P. Hrelia, Sulforaphane as an inducer of glutathione prevents oxidative stress-induced cell death in a dopaminergic-like neuroblastoma cell line, J. Neurochem. 111 (2009) 1161–1171.
[20] A. Tarozzi, F. Morroni, C. Bolondi, G. Sita, P. Hrelia, A. Djemil, G. Cantelli-Forti, Neuroprotective effects of erucin against 6-hydroxydopamine-induced oxidative damage in a dopaminergic-like neuroblastoma cell line, Int. J. Mol. Sci. 13 (2012) 10899–10910.
[21] Q. Zhou, B. Chen, X. Wang, L. Wu, Y. Yang, X. Cheng, Z. Hu, X. Cai, J. Yang, X. Sun, Sulforaphane protects against rotenone-induced neurotoxicity in vivo: involvement of the mTOR, Nrf2, and autophagy pathways, Sci. Rep. 6 (2016) 32206.
[22] A. Tarozzi, C. Angeloni, M. Malaguti, F. Morroni, S. Hrelia, P. Hrelia, Sulforaphane as a Potential Protective Phytochemical against Neurodegenerative diseases, Oxidative Med. Cell. Longev. (2013) 2013.
[23] D. Carnevale, R. De Simone, L. Minghetti, Microglia-neuron interaction in inflammatory and degenerative diseases: role of cholinergic and noradrenergic systems, CNS Neurol. Disord. - Drug Targets 6 (2007) 388–397.
[24] D.V. Hansen, J.E. Hanson, M. Sheng, Microglia in Alzheimer's disease, J. Cell Biol. 217 (2018) 459.
[25] M. Colonna, O. Butovsky, Microglia function in the central nervous system during health and neurodegeneration, Annu. Rev. Immunol. 35 (2017) 441–468.
[26] S.A. Liddelow, K.A. Guttenplan, L.E. Clarke, F.C. Bennett, C.J. Bohlen, L. Schirmer, M.L. Bennett, A.E. Münch, W.-S. Chung, T.C. Peterson, Neurotoxic reactive astrocytes are induced by activated microglia, Nature 541 (2017) 481.
[27] Z. Chen, M. Digiacomo, Y. Tu, Q. Gu, S. Wang, X. Yang, J. Chu, Q. Chen, Y. Han, J. Chen, Discovery of novel rivastigmine-hydroxycinnamic acid hybrids as multi-targeted agents for Alzheimer's disease, Eur. J. Med. Chem. 125 (2017) 784–792.
[28] A. Martelli, V. Citi, V. Calderone, Vascular effects of H 2 S-donors: fluorimetric detection of H 2 S generation and ion channel activation in human aortic smooth muscle cells, in: Vascular Effects of Hydrogen Sulfide,, Springer, 2019, pp. 79–87.
[29] A. Martelli, L. Testai, V. Citi, A. Marino, F.G. Bellagambi, S. Ghimenti, M.C. Breschi, V. Calderone, Pharmacological characterization of the vascular effects of aryl isothiocyanates: is hydrogen sulfide the real player? Vasc. Pharmacol. 60 (2014) 32–41.
[30] V. Citi, A. Martelli, L. Testai, A. Marino, M.C. Breschi, V. Calderone, Hydrogen sulfide releasing capacity of natural isothiocyanates: is it a reliable explanation for the multiple biological effects of Brassicaceae? Planta Med. 80 (2014) 610–613.
[31] E. Lucarini, L. Micheli, E. Trallori, V. Citi, A. Martelli, L. Testai, G.R. De Nicola, R. Iori, V. Calderone, C. Ghelardini, Effect of glucoraphanin and sulforaphane against chemotherapy-induced neuropathic pain: Kv7 potassium channels modulation by H2S release in vivo, Phytother Res. 32 (2018) 2226–2234.
[32] A. Martelli, E. Piragine, V. Citi, L. Testai, E. Pagnotta, L. Ugolini, L. Lazzeri, L. Di Cesare Mannelli, O.L. Manzo, M. Bucci, Erucin exhibits vasorelaxing effects and antihypertensive activity by H2S-releasing properties, Br. J. Pharmacol. (2019) 1–12.
[33] V. Citi, E. Piragine, E. Pagnotta, L. Ugolini, L. Di Cesare Mannelli, L. Testai, C. Ghelardini, L. Lazzeri, V. Calderone, A. Martelli, Anticancer properties of erucin, an H2S-releasing isothiocyanate, on human pancreatic adenocarcinoma cells (AsPC-1), Phytother Res. 33 (2019) 845–855.
[34] F. Regen, J. Hellmann-Regen, E. Costantini, M. Reale, Neuroinflammation and Alzheimer's disease: implications for microglial activation, Curr. Alzheimer Res. 14 (2017) 1140–1148.
[35] F. Morroni, G. Sita, A. Djemil, M. D'Amico, L. Pruccoli, G. Cantelli-Forti, P. Hrelia, A. Tarozzi, Comparison of adaptive neuroprotective mechanisms of sulforaphane and its interconversion product erucin in in vitro and in vivo models of Parkinson's Disease 66 (2018) 856–865.
[36] V. Calabrese, C. Cornelius, A.T. Dinkova-Kostova, E.J. Calabrese, M.P. Mattson, Cellular stress responses, the hormesis paradigm, and vitagenes: novel targets for therapeutic intervention in neurodegenerative disorders, Antioxidants Redox Signal. 13 (2010) 1763–1811.
[37] Y. Shao, Z. Chen, L. Wu, Oxidative stress effects of soluble sulfide on human

hepatocyte cell line LO2, Int. J. Environ. Res. Public Health 16 (2019) 1662.
[38] S. Fortunato, C. Lenzi, C. Granchi, V. Citi, A. Martelli, V. Calderone, S. Di Pietro, G. Signore, V. Di Bussolo, F. Minutolo, First examples of H2S-releasing glycoconjugates: stereoselective synthesis and anticancer activities, Bioconjug. Chem. (2019).
[39] E. Barresi, G. Nesi, V. Citi, E. Piragine, I. Piano, S. Taliani, F. Da Settimo, S. Rapposelli, L. Testai, M.C. Breschi, Iminothioethers as hydrogen sulfide donors: from the gasotransmitter release to the vascular effects, J. Med. Chem. 60 (2017) 7512–7523.
[40] K.S.T. Dias, C.T. de Paula, T. dos Santos, I.N. Souza, M.S. Boni, M.J. Guimarães, F.M. da Silva, N.G. Castro, G.A. Neves, C.C. Veloso, Design, synthesis and evaluation of novel feruloyl-donepezil hybrids as potential multitarget drugs for the treatment of Alzheimer's disease, Eur. J. Med. Chem. 130 (2017) 440–457.
[41] A. Rampa, M. Bartolini, L. Pruccoli, M. Naldi, I. Iriepa, I. Moraleda, F. Belluti, S. Gobbi, A. Tarozzi, A. Bisi, Exploiting the chalcone scaffold to develop multifunctional agents for Alzheimer's disease, Molecules 23 (2018) 1902.
[42] A. Rampa, S. Montanari, L. Pruccoli, M. Bartolini, F. Falchi, A. Feoli, A. Cavalli, F. Belluti, S. Gobbi, A. Tarozzi, Chalcone-based carbamates for Alzheimer's disease treatment, Future Med. Chem. 9 (2017) 749–764.
[43] S. Montanari, M. Bartolini, P. Neviani, F. Belluti, S. Gobbi, L. Pruccoli, A. Tarozzi, F. Falchi, V. Andrisano, P. Miszta, Multitarget strategy to address Alzheimer's disease: design, synthesis, biological evaluation, and computational studies of coumarin-based derivatives, ChemMedChem 11 (2016) 1296–1308.
[44] F.P.D. Viegas, M. de Freitas Silva, M.D. da Rocha, M.R. Castelli, M.M. Riquiel, R.P. Machado, S.M. Vaz, L.M.S. de Lima, K.C. Mancini, P.C.M. de Oliveira, Design, synthesis and pharmacological evaluation of N-benzyl-piperidinyl-aryl-acylhydrazone derivatives as donepezil hybrids: discovery of novel multi-target anti-alzheimer prototype drug candidates, Eur. J. Med. Chem. 147 (2018) 48–65.